Iranian Journal of Organic Chemistry Vol. 9, No. 2(2017) 2045-2055

Quantum-mechanical investigation of 1-benzyl-1,4,7,10-tetraazacyclododecane: a density functional theory (DFT) treatment

Mehdi Nabati*

Chemistry Department, Faculty of Science, Azarbaijan Shahid Madani University, Tabriz, Iran

Received: February 2017; Revised: March 2017; Accepted: April 2017

Abstract: In the present paper, the density functional theory (DFT) method has been done to study the structural properties, reactivity and UV-Vis, IR and NMR spectral properties of the 1-benzyl-1,4,7,10-tetraazacyclododecane molecule by using the B3LYP functional and 6-31G(d,p) basis set, as well as the optimized structure. The investigation of the structural parameters (bond lengths, bond angles, dihedral angles and bond orders) and frontier molecular orbitals (FMOs) of the compound indicates that the nitrogen atoms of the structure are more reactive than other regions of the molecule and they can attack to the various electron-poor reactants. And also, the UV-Vis, IR and NMR study of the molecule shows the high accuracy of the used computational method.

Keywords: 1-Benzyl-1,4,7,10-tetraazacyclododecane, DFT study, Nuclear medicine, Quantum-mechanical study, Radiopharmaceutical.

Introduction

Radiopharmacology or medicinal radiochemistry is radiochemistry applied to medicine and thus the pharmacology of radiopharmaceuticals (medicinal radio-compounds, that is, pharmaceutical drugs that are radioactive). Radiopharmaceuticals are used in the field of nuclear medicine as radioactive tracers in medical imaging and in therapy for many diseases (for example, brachytherapy). Many radiopharmaceuticals use technetium-99m (Tc-99m) which has many useful properties as a gamma-emitting tracer nuclide. In the book *Technetium* a total of 31 different radiopharmaceuticals based on Tc-99m are listed for imaging and functional studies of the brain, myocardium, thyroid, lungs, liver, gallbladder, kidneys, skeleton, blood and tumors [1-3].

Nuclear medicine is a medical specialty involving the application of radioactive substances in the diagnosis and treatment of disease.

*Corresponding author. Tel: +98 (413) 4327501, Fax: +98 (413) 4327501, E-mail: mnabati@ymail.com

Nuclear medicine, in a sense, is "radiology done inside out" or "endoradiology" because it records radiation emitting from within the body rather than radiation that is generated by external sources like X-rays. In addition, nuclear medicine scans differ from radiology as the emphasis is not on imaging anatomy but the function and for such reason; it is called a physiological imaging modality. Single Photon Emission Computed Tomography or SPECT and Positron Emission Tomography or PET scans are the two most common imaging modalities in nuclear medicine [4-6]. Despite the advances in medical sciences, cancer is still a leading cause of death worldwide. The World Health Organization reported that, in developed countries, cancer is the second leading cause of death, being only surpassed by cardiovascular diseases. Nevertheless, during recent decades, remarkable insights into the cell and molecular biology of malignancies have been acquired, and a myriad of differences in the biological make-up of cancers compared with their healthy-tissue counterparts have been catalogued. The increasing

with D_2O) and 7.3- 7.6 ppm due to CH_3, OCH_2, NH_2 knowledge generated by such achievements has led to the identification of several biomarkers, and some of them have been considered as potential targets for *in vivo* molecular imaging and/or therapeutic purposes. Among others, antigens, membrane receptors and enzymes have been considered as interesting biomarkers, since they play important roles in pathological processes, being in most cases overexpressed compared to endogenous expression levels [1-7].

In recent years, many acyclic and cyclic polyamine ligands were prepared and labeled with radionuclides as diagnostic and therapy applications for cancer disease [8]. Unfortunately, theoretical investigation of the structural properties of these ligands hasn't been done up to now. The present paper studies the structural properties of 1-benzyl-1,4,7,10-tetraazacyclododecane ligand by quantum mechanical (QM) computations.

Results and discussion

Structural properties study of 1-benzyl-1,4,7,10-tetraazacyclododecane:

In the present research work, the 1-benzyl-1,4,7,10-tetraazacyclododecane molecule was investigated theoretically. The studied compound with atom numbering is shown in Scheme **1**. This molecule was optimized by quantum mechanical (QM) computational method at B3LYP/6-31G(d,p) level of theory. The optimized structure of the compound is shown in Figure **1**. The bond lengths, bond angles and dihedral angles data of the optimized structure of the compound are listed in Table **1**. As results from the Table **1**, the length of the aliphatic N-C and C-C bonds of the structure varies in 1.46-1.47 Å and 1.45-1.55 Å ranges, respectively. Also, the length of the aromatic C-C bonds of the benzyl ring in the structure is about 1.4 Å. From the bond lengths data, we can see the aliphatic C-H bonds are longer than the aromatic C-H bonds. And also, the N-H bonds are smaller than the aliphatic C-H bonds. All angles of the structure (C-C-N, C-N-C and N-C-C angles) vary from 107 to 121 degree. Table **2** indicates the bond orders (B.O.) data of the compound. It can be seen from the data, the BO of the N-H, aliphatic C-H and aromatic C-H bonds is about 0.68, 0.76 and 0.77, respectively.

It can be deduced from these data, the N-H bonds have acidic property. Also, we can see that the N-C, aliphatic C-C and aromatic C-C bond orders are in the ranges of 0.80-0.83, 0.82-0.84 and 1.13-1.15, respectively. The N4-C5 bond has the lowest bond order among all N-C bonds.

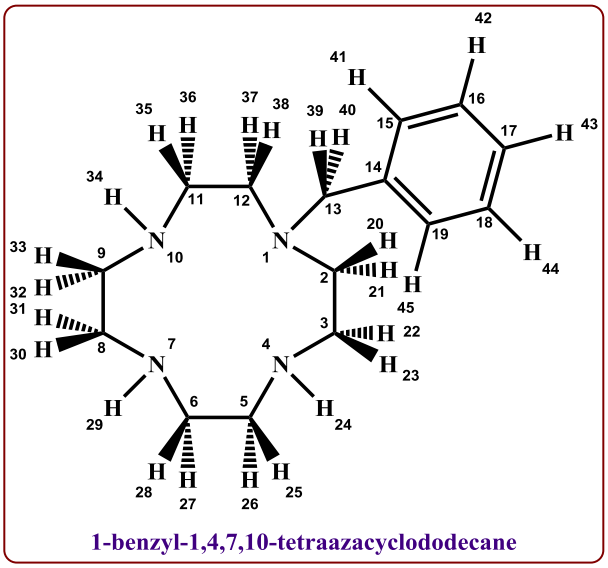

Scheme 1. The structure of the studied molecule.

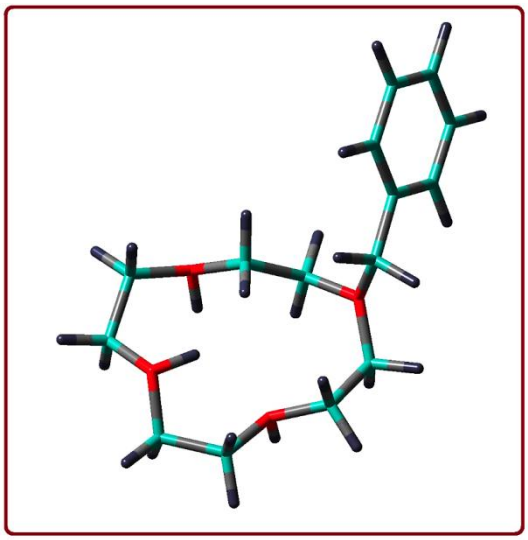

Figure 1. The optimized structure of 1-benzyl-1,4,7,10-tetraazacyclododecane ligand.

Table 1. Bond lengths, bond angles and dihedral angles data of the studied molecule.

Bonds	**Bond length (Angstrom)**	**Bond angle**	**Angle (degree)**
N1-C2	1.457	N1-C2-C3	120.845
C2-C3	1.549	C2-C3-N4	112.214
C3-N4	1.460	C3-N4-C5	117.206
N4-C5	1.469	N4-C5-C6	109.318
C5-C6	1.539	C5-C6-N7	106.965
C6-N7	1.458	C6-N7-C8	117.829
N7-C8	1.459	N7-C8-C9	109.905
C8-C9	1.451	C8-C9-N10	114.128
C9-N10	1.471	C9-N10-C11	117.480
N10-C11	1.467	N10-C11-C12	110.075
C11-C12	1.547	C11-C12-N1	116.546
C12-N1	1.464	C12-N1-C2	118.856
N1-C13	1.456	C12-N1-C13	116.319
C13-H39	1.105	N1-C13-C14	113.298
C13-H40	1.099	C13-C14-C15	120.607
C13-C14	1.522	C14-C15-C16	120.819
C14-C15	1.399	C15-C16-C17	120.027
C15-C16	1.397	C16-C17-C18	119.585
C16-C17	1.395	C17-C18-C19	120.222
C17-C18	1.397	C18-C19-C14	120.634
C18-C19	1.394	C15-C14-C19	118.713

C19-C14	1.401	N1-C2-C3-N4	75.596
C15-H41	1.088	C2-C3-N4-C5	176.501
C16-H42	1.086	C3-N4-C5-C6	154.870
C17-H43	1.086	N4-C5-C6-N7	56.779
C18-H44	1.087	C5-C6-N7-C8	150.766
C19-H45	1.086	C6-N7-C8-C9	149.258
C2-H20	1.098	N7-C8-C9-N10	60.601
C2-H21	1.100	C8-C9-N10-C11	93.268
C3-H22	1.108	C9-N10-C11-C12	165.254
C3-H23	1.097	N10-C11-C12-N1	154.632
N4-H24	1.017	C11-C12-N1-C2	95.890
C5-H25	1.096	C12-N1-C2-C3	74.736
C5-H26	1.102	C12-N1-C13-C14	62.318
C6-H27	1.109	N1-C13-C14-C15	138.972
C6-H28	1.098	C2-N1-C13-C14	150.002
N7-H29	1.015	C2-C3-N4-H24	57.735
C8-H30	1.100	C6-C5-N4-H24	79.387
C8-H31	1.110	C5-C6-N7-H29	35.061
C9-H32	1.098	C9-C8-N7-H29	35.386
C9-H33	1.096	C8-C9-N10-H34	32.111
N10-H34	1.017	C12-C11-N10-H34	40.081
C11-H35	1.101	C13-N1-C2-H20	49.982
C11-H36	1.098	C13-N1-C2-H21	163.345
C12-H37	1.097	C13-N1-C12-H37	172.604
C12-H38	1.096	C13-N1-C12-H38	72.654

Table 2. Bond orders (B.O.) data of the studied molecule.

Bonds	**Bond orders**	**Bonds**	**Bond orders**
N1-C2	0.832	C16-H42	0.774
C2-C3	0.834	C17-H43	0.774
C3-N4	0.808	C18-H44	0.774
N4-C5	0.798	C19-H45	0.773
C5-C6	0.839	C2-H20	0.760
C6-N7	0.809	C2-H21	0.761
N7-C8	0.807	C3-H22	0.754
C8-C9	0.844	C3-H23	0.761

C9-N10	0.805	N4-H24	0.679
N10-C11	0.808	C5-H25	0.761
C11-C12	0.821	C5-H26	0.762
C12-N1	0.812	C6-H27	0.755
N1-C13	0.814	C6-H28	0.759
C13-H39	0.754	N7-H29	0.683
C13-H40	0.758	C8-H30	0.756
C13-C14	0.862	C8-H31	0.755
C14-C15	1.142	C9-H32	0.758
C15-C16	1.138	C9-H33	0.762
C16-C17	1.143	N10-H34	0.686
C17-C18	1.136	C11-H35	0.764
C18-C19	1.147	C11-H36	0.758
C19-C14	1.132	C12-H37	0.765
C15-H41	0.773	C12-H38	0.758

Reactivity prediction of 1-benzyl-1,4,7,10-tetraazacyclododecane:

In this section of research work, the molecular orbital (MO) theory of the studied molecule is explored. In chemistry, frontier molecular orbital (FMO) theory is an application of MO theory describing HOMO/LUMO interactions [9]. The images of the frontier molecular orbitals of this compound are shown in Figure **2**. The Figure **2** shows that the nitrogen atoms and benzene ring are the electron-rich and electron-poor sites of the molecule. So, the nitrogen atoms can attack to the electron-poor reactants. From the calculations, the energies of the HOMO and LUMO are -5.37 and 0.05 eV, respectively. The HOMO/LUMO energies gap indicates that this molecule is a stable compound. The energies of the virtual and occupied orbitals of the compound are shown in density of states (DOS) graph (Figure **3**). This graph indicates that the states of the unoccupied orbitals are more than the occupied orbitals. So, this compound can do the nucleophilic reactions better than the electrophilic reactions.

The molecular electrostatic potential (MEP) at a given point p(x,y,z) in the vicinity of a molecule is the force

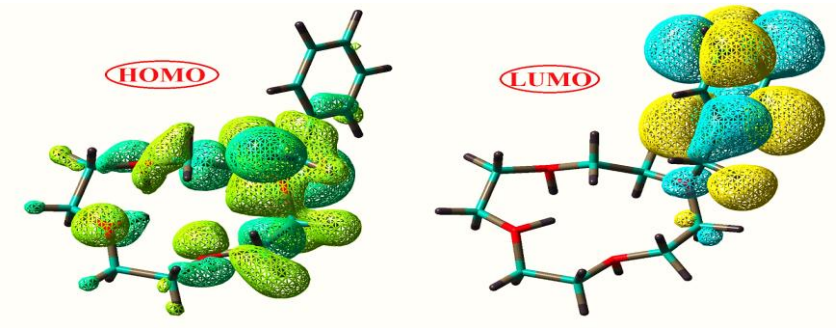

Figure 2. The frontier molecular orbitals of 1-benzyl-1,4,7,10-tetraazacyclododecane ligand.

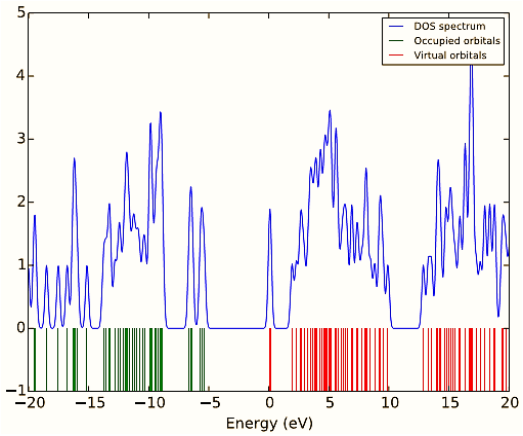

Figure 3. The density of states (DOS) graph of 1-benzyl-1,4,7,10-tetraazacyclododecane ligand.

acting on a positive test charge (a proton) located at p through the electrical charge cloud generated through the molecules electrons and nuclei. Despite the fact that the molecular charge distribution remains unperturbed through the external test charge (no polarization occurs) the electrostatic potential of a molecule is still a good guide in assessing the molecules reactivity towards positively or negatively charged reactants. The MEP is typically visualized through mapping its values onto the surface reflecting the molecules boundaries [10-12]. Figure **4** shows the molecular electrostatic potential (MEP) graph of the molecule. In this molecule, the colors have been chosen such that regions of attractive potential appear in red and those of repulsive potential appear in green. It can be seen from the Figure **4** that the regions containing the nitrogen atoms are the electron-rich sites of the molecule. So, these regions can participate in nucleophilic reactions.

UV-Vis, IR and NMR spectra prediction of 1-benzyl-1,4,7,10-tetraazacyclododecane

There are several spectroscopic techniques which can be used to identify organic molecules: infrared (IR), mass spectroscopy (MS) UV-Visible spectroscopy (UV-Vis) and nuclear magnetic resonance (NMR). IR, NMR and UV-Vis spectroscopy are based on observing the frequencies of electromagnetic radiation absorbed and emitted by molecules [13].

UV/Vis Spectroscopy uses ultraviolet and/or visible light to examine the electronic properties of molecules. Irradiating a molecule with UV or Visible light of a specific wavelength can cause the electrons in a molecule to transition to an excited state [14]. The UV-Vis spectrum of the studied molecule is shown in Figure **5**. In the UV-Vis spectrum, the peak at wavelength 267.985 nm with energy 37315.498 cm^{-1} is related to the HOMO to LUMO transition. The other transition (HOMO to LUMO+1) takes place at wavelength 259.939 nm with energy 38470.492 cm^{-1}.

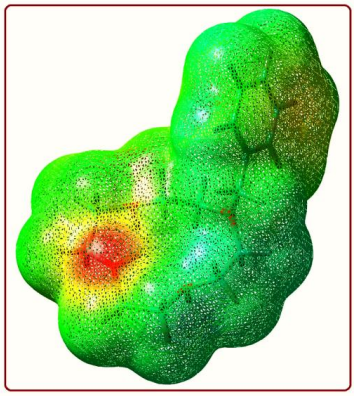

Figure 4. The molecular electrostatic potential (MEP) graph of 1-benzyl-1,4,7,10-tetraazacyclododecane ligand.

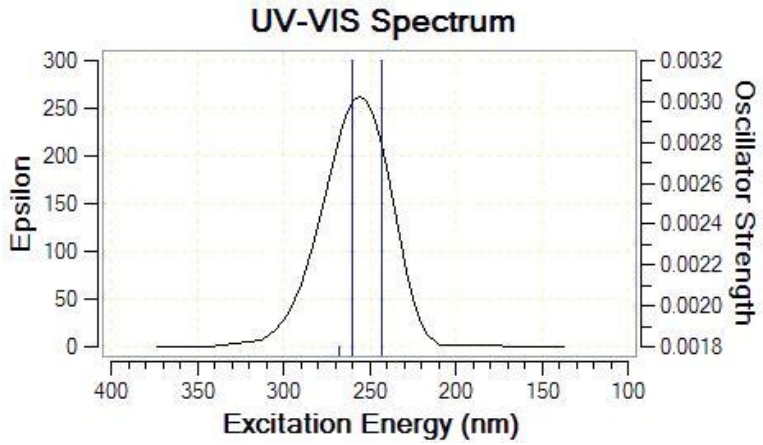

Figure 5. The UV-Vis spectrum of 1-benzyl-1,4,7,10-tetraazacyclododecane ligand.

Also, the HOMO-1 to LUMO transition is shown at wavelength 242.629 nm with energy 41215.216 cm^{-1}.

Infrared (IR) Spectroscopy is the analysis of infrared light interacting with a molecule. This can be analyzed in three ways by measuring absorption, emission and reflection. The main use of this technique is in organic and inorganic chemistry. It is used by chemists to determine functional groups in molecules. IR Spectroscopy measures the vibrations of atoms, and based on this it is possible to determine the functional groups. Generally, stronger bonds and light atoms will vibrate at a high stretching frequency (wavenumber) [14-16]. Figure **6** indicates the IR spectrum of the studied molecule. IR [Harmonic frequencies (cm^{-1}), intensities (KM/Mole)]: 21.2746 (0.0865), 26.2964 (0.0919), 34.6213 (0.3080), 51.9467 (2.1214), 89.5578 (0.6671), 96.4449 (0.3185), 112.5891 (0.4832), 164.5732 (0.6081), 166.5673 (2.8833), 185.5802 (3.6067), 208.2239 (1.7609), 221.5883 (1.5545), 227.4550 (0.5649), 233.4024 (4.2379), 289.6772 (3.3869), 315.8404 (0.3094), 329.5120 (0.4825), 349.0910 (1.2646), 377.4697 (1.0589), 404.9973 (1.6957), 419.9198 (0.1600), 436.7534 (4.3759), 453.7310 (22.7924), 496.1511 (4.5475), 513.0619

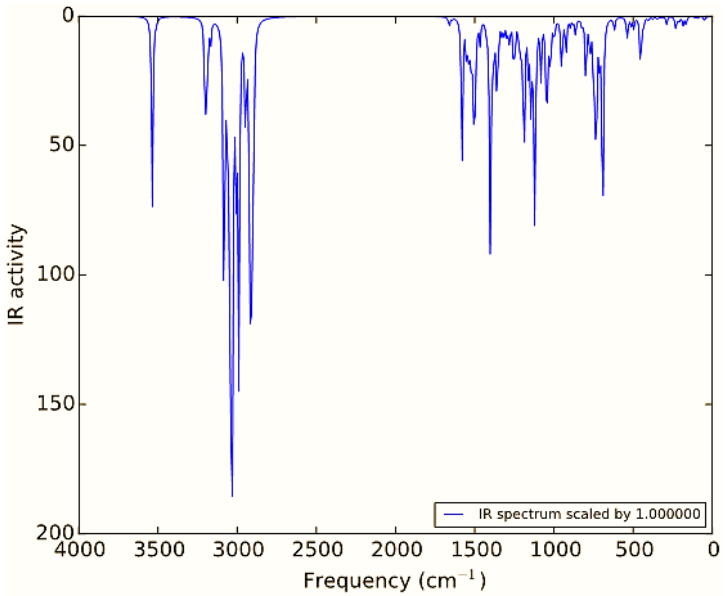

Figure 6. The IR spectrum of 1-benzyl-1,4,7,10-tetraazacyclododecane ligand.

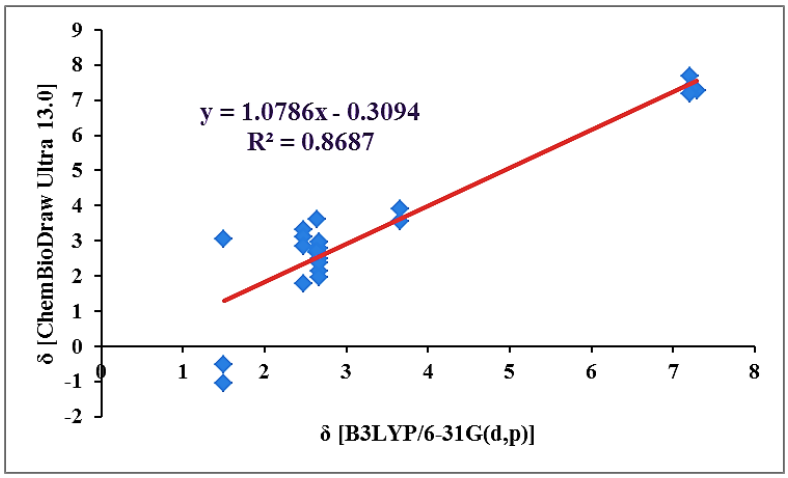

Figure 7. The relationship between theoretical and experimental ^{1}H chemical shifts of the studied structure.

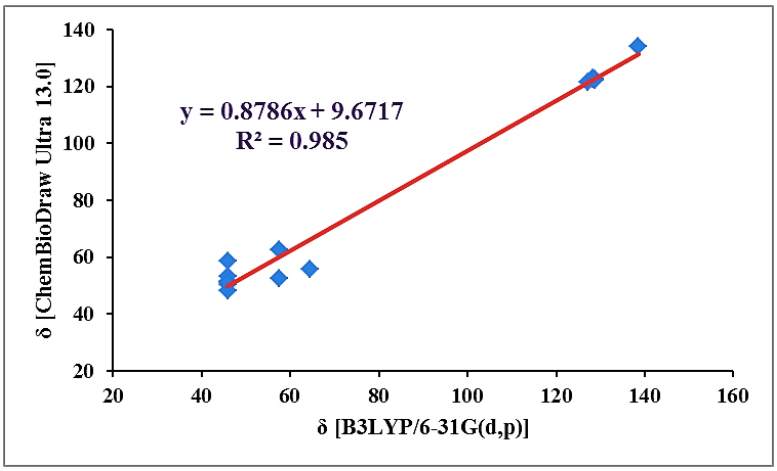

Figure 8. The relationship between theoretical and experimental ^{13}C chemical shifts of the studied structure.

Table 3. The ^{1}H and ^{13}C chemical shifts of the studied molecule.

Nucleus	Chemical Shift (ppm)	
	Theoretical chemical shifts ($\delta = \delta_{TMS} - \delta'$)	**δ (Chemical shifts from ChemBioDraw Ultra 13.0)**
H-20	1.787	2.48
H-21	3.331	2.48
H-22	2.772	2.65
H-23	3.598	2.65
H-24	-1.064	1.50
H-25	2.784	2.67

H-26	2.487	2.67
H-27	2.956	2.67
H-28	2.143	2.67
H-29	3.057	1.50
H-30	1.967	2.67
H-31	2.647	2.67
H-32	2.360	2.67
H-33	2.958	2.67
H-34	-0.533	1.50
H-35	2.660	2.65
H-36	2.691	2.65
H-37	3.100	2.48
H-38	2.858	2.48
H-39	3.553	3.66
H-40	3.910	3.66
H-41	7.698	7.21
H-42	7.378	7.23
H-43	7.278	7.29
H-44	7.323	7.23
H-45	7.195	7.21
C-2	52.404	57.50
C-3	51.554	45.90
C-5	48.156	46.00
C-6	58.644	46.00
C-8	53.368	46.00
C-9	50.536	46.00
C-11	51.120	45.90
C-12	62.577	57.50
C-13	55.889	64.40
C-14	134.083	138.60
C-15	122.698	128.80
C-16	122.951	128.40
C-17	121.622	127.20
C-18	122.575	128.40
C-19	122.366	128.80

(3.1366), 531.6274 (1.4073), 539.2603 (8.6859), 619.2745 (5.4278), 634.8498 (0.1937), 692.6227 (96.0225), 712.9220 (12.5541), 733.8805 (61.5598), 749.0656 (30.3665), 772.8222 (14.6090), 798.9250 (27.4159), 823.1979 (3.3635), 843.3510 (0.3089), 863.6286 (6.9624), 865.7687 (0.2806), 879.8290 (1.9230), 897.7514 (3.2615), 923.4157 (6.9510), 924.2960 (7.8041), 949.5116 (12.6023), 955.0639 (11.6290), 976.7782 (0.4151), 995.0582 (4.5456), 1002.7256 (3.8126), 1016.3842 (0.1337), 1019.9339 (5.8795), 1023.8810 (14.5459), 1037.9506 (6.3844), 1046.0997 (43.9154), 1054.9628 (3.8949), 1082.5099 (22.4851), 1105.8341 (3.6770), 1120.9017 (81.2416), 1131.8397 (3.7439), 1135.3000 (9.0586), 1146.3738 (31.6429), 1162.1752 (17.6816), 1185.4692 (0.2431), 1185.8619 (5.3624), 1189.5683 (55.7609), 1199.5932 (2.6476), 1207.3845 (12.3824), 1219.5900 (5.3221), 1222.9207 (3.7903), 1246.3015 (12.5843), 1255.9510 (15.9860), 1280.3825 (9.6668), 1291.0469 (2.6550), 1299.8269 (5.4652), 1315.2027 (5.2614), 1328.7585 (5.9536), 1350.0053 (8.3751), 1358.8908 (1.2891), 1359.9989 (23.5022), 1364.6967 (6.1486), 1377.0086 (4.9766), 1378.8167 (3.4331), 1390.9845 (20.2577), 1402.3828 (51.1968), 1403.8630 (37.6105), 1413.6269 (1.5517), 1416.3067 (1.6346), 1428.8804 (3.1053), 1467.0391 (9.2114), 1486.8088 (2.0905), 1490.6990 (0.7803), 1496.2918 (13.4639), 1498.8473 (17.7301), 1503.4001 (1.5564), 1508.4783 (31.3788), 1511.7767 (3.2456), 1521.8318 (6.1517), 1526.8483 (13.3638), 1538.2430 (9.1117), 1541.3802 (3.2671), 1552.3034 (16.7453), 1580.7030 (59.4510), 1642.6113 (0.6638), 1661.7588 (3.8253), 2895.9058 (36.7001), 2906.8901 (116.8029), 2919.7947 (108.3166), 2947.1564 (44.4958), 2988.8438 (100.2493), 2991.5072 (42.3577), 3006.4959 (51.9115), 3019.8050 (12.2248), 3030.5433 (82.6062), 3031.2773 (63.6538), 3036.0757 (31.1582), 3040.7345 (60.4687), 3042.8548 (65.1531), 3050.8966 (38.8441), 3064.5708 (31.8551), 3082.7416 (36.4035), 3083.3705 (50.9303), 3084.3635 (36.3200), 3167.3444 (8.7155), 3176.9895 (0.0957), 3187.2925 (19.1200), 3196.8277 (27.8567), 3204.5174 (20.8579), 3509.0411 (0.4071), 3512.3331 (1.4202) and 3535.8332 (75.0722).

Nuclear magnetic resonance spectroscopy, most commonly known as NMR spectroscopy, is a research technique that exploits the magnetic properties of certain atomic nuclei. This type of spectroscopy determines the physical and chemical properties of atoms or the molecules in which they are contained. The NMR technique is a good method for identification of the structure of the organic compounds [16-19]. The ^{1}H and ^{13}C chemical shifts of the studied molecule are listed in Table **3**. The theoretical chemical shifts data is compared to the experimental values. The Figures **7** and **8** indicate the comparison between the theoretical and experimental ^{1}H and ^{13}C chemical shifts of the molecular structure at studied computational method. The differences between calculations and experiment are partly not systematic; the linear regressions are characterized by rather large correlation coefficients. In fact, two approaches were adopted in these linear fits. First, all C atoms were considered in the fit; second, the fitness of the H atoms is less than the C atoms. Representing the relationship between the experimental and theoretical results further indicates that theories are misleading in estimating the chemical shift values for the most deshielded H34 and H24 atoms.

Computational method:

In this paper, all calculations are performed with the GAUSSIAN 03 program package. Standard quantum chemical density functional theory (DFT) method is used at B3LYP level of theory. For DFT calculations the Beck's hybrid one-parameter and three-parameter functional are employed, using the LYP correlation, as implemented by Adamo and Barone, as well as the Lee-Yang-Parr non-local correlation functional B3LYP, with the 6-31G(d,p) basis set.

Conclusions

In the present work, the 1-benzyl-1,4,7,10-tetraazacyclododecane compound was computed by density functional theory (DFT) method at B3LYP/6-31G(d,p) level of theory. In first step, the molecular structure of the compound was optimized at mentioned computational method. The bond lengths, bond angles, dihedral angles and bond orders of the structure studied theoretically. The frontier molecular orbitals (FMOs) investigation on the structure shows that the nitrogen atoms can attack to the various electron-poor reactants. Finally, the UV-Vis, IR and NMR study of the molecule indicates the high accuracy of the used computational method in this research work.

Acknowledgments

The present research work was supported by the Azarbaijan Shahid Madani University (ASMU), Tabriz, Iran. Also, the corresponding author is grateful to Dr. Hojjatollah Salehi and Mr. Hossein Abbasi for providing valuable suggestions.

References

[1] Fallahi, B.; Esmaeili, A.; Beiki, D.; Oveisgharan, S.; Noorollahi-Moghaddam, H.; Erfani, M.; Tafakhori, A.; Rohani, M.; Fard-Esfahani, A.; Emami-Ardekani, A.; Geramifar, P.; Eftekhari, M. *Ann. Nucl. Med.*, **2016**, *30*, 153-162.
[2] Erfani, M.; TShafiei, M. *Nucl. Med. Biol.*, **2014**, *30*, 317-321.
[3] Erfani, M.; TShafiei, M.; Charkhlooie, G.; Goudarzi, M. *Iran J. Nucl. Med.*, **2015**, *23*, 15-20.
[4] Kushner, S. A.; McElgin, W. T.; Kung, M.; Mozley, P. D.; Plossl, K.; Meegalla, S. K.; Mu, M.; Dresel, S.; Vessotskie, J. M.; Lexow, N.; Kung, H. F. *J. Nucl. Med.*, **1999**, *40*, 150-158.
[5] Toth, G.; Szakonyi, Z.; Kanyo, B.; Fulop, F.; Jancso, G.; Pavics, L. *J. Label. Compd. Radiopharm.*, **2003**, *46*, 1067-1073.
[6] Abou El Ella, D. A.; Ghorab, M. M.; Heiba, H. I.; Soliman, A. M. *Med. Chem. Res.*, **2012**, *21*, 2395-2407.
[7] Ritz, M. C.; Lamb, R. J.; Goldberg, S. R.; Kuhar, M. J. *Science*, **1987**, *237*, 1219-1223.
[8] Correia, J. D. G.; Paulo, A.; Raposinho, P. D.; Santos, I. *Dalton Trans.*, **2011**, *40*, 6144-6167.
[9] Nabati, M. *J. Phys. Theor. Chem. IAU Iran*, **2015**, *12*, 325-338.
[10] Nabati, M.; Mahkam, M.; Atani, Y. G. *J. Phys. Theor. Chem. IAU Iran*, **2016**, *13*, 35-59.
[11] Nabati, M.; Mahkam, M. *Org. Chem. Res.*, **2016**, *2*, 70-80.
[12] Nabati, M. *Iran. J. Org. Chem.*, **2016**, *8*, 1703-1716.
[13] Nabati, M. *J. Phys. Theor. Chem. IAU Iran*, **2016**, *13*, 133-146.
[14] Nabati, M.; Mahkam, M. *J. Phys. Theor. Chem. IAU Iran*, **2015**, *12*, 33-43.
[15] Nabati, M.; Mahkam, M. *Silicon*, **2016**, *8*, 461-465.
[16] Nabati, M.; Hojjati, M. *Iran. J. Org. Chem.*, **2016**, *8*, 1777-1787.
[17] Nabati, M.; Mahkam, M. *Iran. J. Org. Chem.*, **2015**, *7*, 1463-1472.
[18] Nabati, M. *Iran. J. Org. Chem.*, **2015**, *7*, 1631-1640.
[19] Nabati, M.; Mahkam, M. *J. Phys. Theor. Chem. IAU Iran*, **2015**, *12*, 121-136.
[20] Frisch, M. J.; Trucks, G. W.; Schlegel, H. B.; Scuseria, G. E.; Robb, M. A.; Cheeseman, J. R.; Montgomery Jr., J. A.; Vreven, T.; Kudin, K. N.; Burant, J. C.; Millam, J. M.; Iyengar, S. S.; Tomasi, J.; Barone, V.; Mennucci, B.; Cossi, M.; Scalmani, G.; Rega, N.; Petersson, G. A.; Nakatsuji, H.; Hada, M.; Ehara, M.; Toyota, K.; Fukuda, R.; Hasegawa, J.; Ishida, M.; Nakajima, T.; Honda, Y.; Kitao, O.; Nakai, H.; Klene, M.; Li, X.; Knox, J. E.; Hratchian, H. P.; Cross, J. B.; Adamo, C.; Jaramillo, J.; Gomperts, R.; Stratmann, R. E.; Yazyev, O.; Austin, A. J.; Cammi, R.; Pomelli, C.; Ochterski, J. W.; Ayala, P. Y.; Morokuma, K.; Voth, G. A.; Salvador, P.; Dannenberg, J. J.; Zakrzewski, V. G.; Dapprich, S.; Daniels, A. D.; Strain, M. C.; Farkas, O.; Malick, D. K.; Rabuck, A. D.; Raghavachari, K.; Foresman, J. B.; Ortiz, J. V.; Cui, Q.; Baboul, A. G.; Clifford, S.; Cioslowski, J.; Stefanov, B. B.; Liu, G.; Liashenko, A; Piskorz, P.; Komaromi, I.; Martin, R. L.; Fox, D. J.; Keith, T.; Al-Laham, M. A.; Peng, C. Y.; Nanayakkara, A.; Challacombe, M.; Gill, P. M. W.; Johnson, B.; Chen, W.; Wong, M. W.; Gonzalez, C.; Pople, J. A. *Gaussian 03. Revision B.01*. Gaussian Inc. Wallingford. CT. **2004**.